In-Trap Spectroscopy of Charge-Bred Radioactive Ions

A. Lennarz,[1,2] A. Grossheim,[2,3] K. G. Leach,[2,3] M. Alanssari,[1] T. Brunner,[2,†] A. Chaudhuri,[2] U. Chowdhury,[2,4] J. R. Crespo López-Urrutia,[5] A. T. Gallant,[2,6] M. Holl,[1] A. A. Kwiatkowski,[2] J. Lassen,[2] T. D. Macdonald,[2,6] B. E. Schultz,[2] S. Seeraji,[3] M. C. Simon,[2] C. Andreoiu,[3] J. Dilling,[2,6] and D. Frekers[1,*]

[1]*Institut für Kernphysik, Westfälische Wilhelms-Universität, 48149 Münster, Germany*

[2]*TRIUMF, Vancouver, British Columbia V6T 2A3, Canada*

[3]*Department of Chemistry, Simon Fraser University, Burnaby, British Columbia V5A 1S6, Canada*

[4]*Department of Physics, University of Manitoba, Winnipeg, Manitoba R3T 2N2, Canada*

[5]*Max Planck Institute for Nuclear Physics, 69117 Heidelberg, Germany*

[6]*Department of Physics and Astronomy, University of British Columbia, Vancouver, British Columbia V6T 1Z1, Canada*

(Received 4 April 2014; published 21 August 2014)

In this Letter, we introduce the concept of in-trap nuclear decay spectroscopy of highly charged radioactive ions and describe its successful application as a novel spectroscopic tool. This is demonstrated by a measurement of the decay properties of radioactive mass $A = 124$ ions (here, ^{124}In and ^{124}Cs) in the electron-beam ion trap of the TITAN facility at TRIUMF. By subjecting the trapped ions to an intense electron beam, the ions are charge bred to high charge states (i.e., equivalent to the removal of N-shell electrons), and an increase of storage times to the level of minutes without significant ion losses is achieved. The present technique opens the venue for precision spectroscopy of low branching ratios and is being developed in the context of measuring electron-capture branching ratios needed for determining the nuclear ground-state properties of the intermediate odd-odd nuclei in double-beta ($\beta\beta$) decay.

DOI: 10.1103/PhysRevLett.113.082502 PACS numbers: 29.30.-h, 23.40.Hc, 29.30.Kv

The storage of radioactive ions in an open-access ion trap opens the potential of observing their decay in a backing-free environment [1,2]. This unique feature is especially advantageous in cases of electron-capture (EC) decays, where measurements of low-energy X-ray photons are required [3]. Recent experiments using a trap-assisted technique for isotopic and isobaric purification have already demonstrated the power of ion traps as a tool for enhanced spectroscopy [4–8]. The trap-assisted technique was applied to EC measurements of ^{100}Tc and ^{116}In, which are the intermediate nuclei in the ^{100}Mo and ^{116}Cd $\beta\beta$ decays [4,8]. However, purified beams still needed to be implanted on a carrier, and the background induced by the orders of magnitude more intense β^- decay made X-ray observation difficult.

The technique of in-trap spectroscopy described in this Letter through a proof-of-principle measurement addresses these limitations by providing backing-free ion-cloud storage inside a 4.5 T magnetic holding field of the electron-beam ion trap (EBIT) [9,10] at the ISAC radioactive ion-beam facility at TRIUMF [11]. The magnetic field causes β particles to spiral out of the trap and away from surrounding detectors if their initial spiral path diameter is less than the radial extent of the central trap electrodes, which in the present case is 7.0 mm [9]. Further, as the spiraling decay electrons or positrons quickly lose energy and change momentum through interactions with the electron beam, the trapped ion cloud, the rest-gas molecules, or through synchrotron radiation, their trapping in the magnetic bottle is largely avoided, and in the case of β^+ decays, annihilation processes are effectively removed from the central trap region [12].

The EBIT is a central part of the TITAN ion trap system at TRIUMF. It consists of a 500 mA electron gun, a drift-tube assembly inside a superconducting magnet in a Helmholtz-like configuration [9], and an electron collector. Its successful operation was demonstrated in recent mass measurements including those where it operated in charge-breeding mode [13–22]. The trap combines a number of advantages for enhanced in-trap nuclear decay spectroscopy. It features seven access ports (Ø 150 and 200 mm) perpendicular to the beam, which permit an unobstructed view into the center of the trap region. The ports are equipped with 0.25 mm vacuum-protecting, high-purity Be windows, which minimize X-ray absorption. Large area (i.e., 2000 mm^2) Si(Li) detectors (thickness 5 mm) are mounted onto each port covering a solid angle acceptance of ≈2%. The detectors were chosen for their highly efficient X-ray detection and their insensitivity to high-energy γ rays. Further, to shield against low-energy Compton backscattered γ rays, the Al housings were covered with a 2 mm thick Cu and 1 mm thick low-activity Pb sleeve [23].

The objective of the present in-trap experiment with radioactive ^{124}Cs ions was to demonstrate the photon or charged particle separation necessary for X-ray spectroscopy of EC processes at low branching ratios and to demonstrate the increase of ion-storage times through charge breeding, thereby allowing decay studies of long-lived radio isotopes.

The use of ^{124}Cs was motivated by its comparatively large EC branch of 7.0% and its half-life of 30.9 s [24]. The total

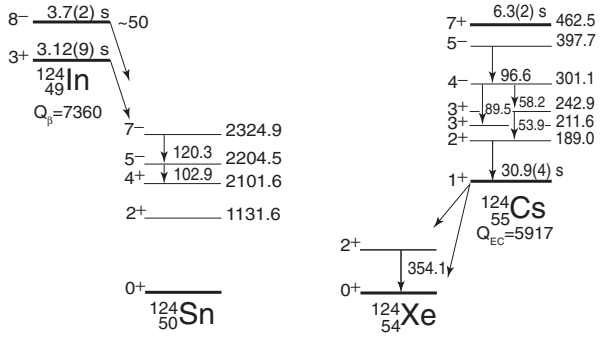

FIG. 1. Decay schemes of ^{124}Cs and ^{124}In and their isomers. Nuclear transitions indicated by arrows are those observed in the present experiment [24].

expected K_α and K_β intensities from the EC/β^+ decays and various conversion processes are reported in Ref. [24] as $I(K_\alpha) = 6.92 \pm 0.15\%$ and $I(K_\beta) = 1.46 \pm 0.05\%$. More details about the ^{124}Cs decay can be found in Ref. [25].

The TRIUMF ISAC facility provided the radioactive beam by bombarding a uranium-carbide (UC) target with a 480 MeV, 9.8 μA proton beam. The radioactive ion beam was accumulated and cooled in the TITAN-RFQ [26] for 1 s, tuned for mass $A = 124$, and transported into the EBIT. It was composed of the ^{124}Cs, $J^\pi = 1^+$ ground state (g.s.), the $J^\pi = 7^+$, 462.5 keV isomer, and of ^{124}In ions, where the latter appeared as the $J^\pi = 8^-$ isomer located at ≈50 keV excitation energy [24]. The high level of ^{124}In contamination was primarily due to the use of the UC production target, because ^{124}In was not detected with a previously used Ta target [27]. The relevant decay schemes of the two nuclei appear in Fig. 1.

The trapped ions in the EBIT were bombarded with a continuous 85 mA electron beam. Two different electron energies (1.5 and 2.0 keV) were chosen during the experiment. At these settings, Cs and In ions were charge bred to configurations corresponding to the removal of the atomic N-shell and parts of the M-shell, or, respectively, to average charge states of $q = 26$–32. Charge-state equilibrium was typically reached after ≈100 ms (see also Refs. [9,22,28]). The continuous electron beam ensures high-equilibrium charge states, and it efficiently reduces ion losses.

Cycle times of 30 s total, consisting of 20 s of trapping time and 10 s of background-measurement time were used over ≈48 h of data taking. Prior to each background-measuring cycle, the trapping potential was lifted to empty the trap. Trap loading and emptying was realized on submillisecond time scales.

Detected X-ray and γ-ray events were time stamped relative to the ion-bunch injection to measure the radioisotope decay times. In Figs. 2(a)–2(c), time-sliced photon-energy spectra between 10 to 140 keV are presented. K_α and K_β X-rays from the three isobars are observed, i.e., ^{124}Cs [from internal conversion (IC) of ^{124m}Cs], ^{124}Xe (from ^{124}Cs EC g.s. decay), and ^{124}Sn (from IC following ^{124m}In β^- decay). Further, γ rays from the ^{124m}Cs decay are

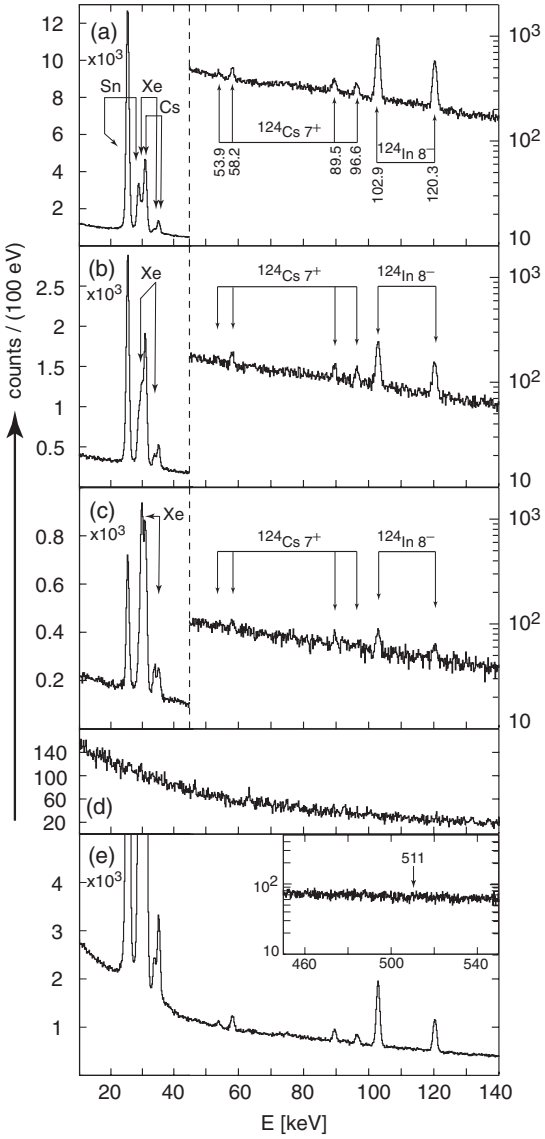

FIG. 2. Photon-energy spectra (10 to 140 keV) for three time intervals: (a) 0–4 s, (b) 8–12 s, and (c) 16–20 s. The spectra show nuclear transitions from ^{124,124m}In (3.7 s) and ^{124m}Cs (6.3 s) decays (logarithmic part) and low-energy X-rays (linear part) with the appearance of Xe X-rays from the (30.9 s) EC decay of the ^{124}Cs ground state. The background during 10 s empty-trap cycles is shown in (d). The spectrum summed over all time intervals of the loaded trap is shown in (e) with the inset indicating the suppression of the 511 keV annihilation γ rays from the β^+-g.s. decay of ^{124}Cs.

observed at 53.9, 58.2, 89.5, and 96.6 keV. Those from the decay of the 3.7 s ^{124m}In appear at 102.9 and 120.3 keV (cf. Fig. 1). The figure shows the different time dependences, as evidenced by the disappearance of the short-lived components of the ^{124m}In and ^{124m}Cs decays and the successively enhanced signature from the 30.9 s ^{124}Cs EC leading to Xe X-rays at $E(K_\alpha) = 29.7$ keV and $E(K_\beta) = 33.7$ keV [29]. The spectrum acquired during the 10 s empty-trap intervals is shown in Fig. 2(d). No signs

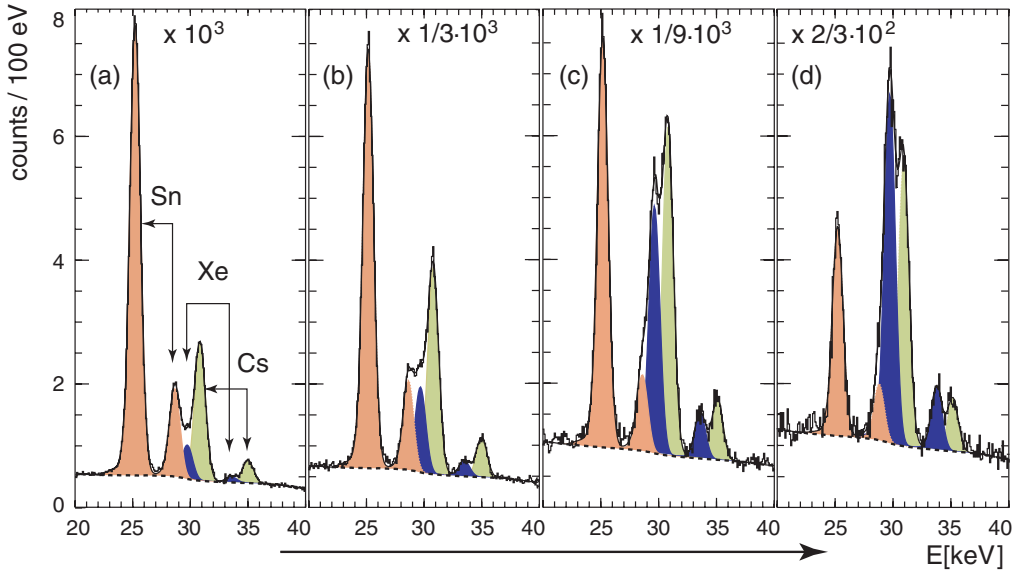

FIG. 3 (color). Time-sliced X-ray spectra. To emphasize the time dependence, the chosen time slices are (a) 0–2 s, (b) 6–8 s, (c) 12–14 s, (d) 18–20 s. Note the different scales. Colored areas are K_α, K_β yields from Sn (red), Xe (blue), and Cs (green). Solid lines describe fits to the data, which are plotted as histograms. Dashed lines describe backgrounds. The comparatively long half-life of the ^{124}Cs (g.s.) results in a relative increase of Xe X-rays at increasing times.

of an accumulated contamination of the trap were observed, indicating the efficient removal of ions from the trap. The spectrum summed over all time intervals of the filled trap is shown in Fig. 2(e). The absence of the 511 keV annihilation line from the ^{124}Cs β^+-decay branch (see inset) demonstrates the efficient spatial separation of X-rays and β^+ particles. One may note that the intensity of the annihilation line is ≈181% compared to ≈8.4% of the X-rays from the ^{124}Cs decay. Folding the spectrum with the Si(Li) photopeak efficiencies at 511 keV of ≈0.04%, one arrives at a 511 keV suppression factor of ≥ 20 given the present statistics.

The efficient ion-bunch injection and trapping is facilitated by the electron beam and was not possible in a previous measurement [27], where 90% of the Cs ions were lost in the first 100 ms after injection. Further, the trapped highly charged ions are confined within a radial extent of 100–200 μm, which is an order of magnitude smaller than in the experiment presented in Ref. [27].

The analysis of the Si(Li) spectra was assisted by a GEANT4 [30] simulation, in which the Si(Li) detectors and the surrounding materials were modeled to determine efficiencies and background functions. Detailed results for the low-energy X-ray region are shown in Fig. 3. Four different time-sliced spectra are described by the various K_α and K_β components of Sn, Xe, and Cs and their time dependences. The simulated background function contains the features of the Compton edges from the 89.4, 96.5, 102.9, and 120.3 keV γ-ray transitions following the 6.3 s decay of the ^{124}Cs(7^+) and the 3.7 s β^- decay of the ^{124}In(8^-) isomers (cf. Fig. 1).

Figure 4 shows decay curves for the summed K_α and K_β transition intensities, from which the half-life for each system is extracted. For the ^{124}Cs isomer and its ground state, these are $T_{1/2} = 6.41 \pm 0.07$ s, and $T_{1/2} = 31 \pm 3$ s, respectively, confirming the literature values [24]. One also notes that the decay curve of the ^{124}Cs ground-state decay is sufficiently well described by a single exponential, since its feeding is too small to be statistically significant. The time dependence of the ^{124}Sn X-rays resulting from the IC process following the ^{124m}In → ^{124}Sn* β decay yields a value of $T_{1/2} = 3.67 \pm 0.03$ s, in agreement with the literature value of $T_{1/2} = 3.7 \pm 0.2$ s [24]. From the relative peak intensities, efficiencies, and half-lives, one evaluates the beam composition for the three radioactive species entering the EBIT, which is ^{124m}Cs 3%, ^{124}Cs 65%, and ^{124m}In 32%.

Highly charged ions exhibit a change in binding energies for the innermost electrons resulting in measurable energy shifts for the K_α and K_β X-rays. Further, since in the present case, charge breeding removed the N-shell electrons, one expects a suppression of the $K_{\beta 2}$ transition and a change of the K_β/K_α ratio.

To identify energy shifts, special attention was given to a precise energy calibration of the spectra, whose accuracy in the low-energy X-ray region was of order 50 eV at an ≈1.1 keV spectral resolution. Because relative energies are less sensitive to possible calibration offsets, energy differences $[E(K_\beta) - E(K_\alpha)]_{q \approx 26-32}$ were extracted and compared with those for neutral atoms $[E(K_\beta) - E(K_\alpha)]_{q=0}$. The extracted energy shifts were around +110 eV with uncertainties of ≈50%. These shifts are consistent with theoretical calculations using the multiconfigurational Dirac-Hartree-Fock code FAC [31]. The positive shifts are caused by the relativistic scaling of the fine-structure splitting, where higher angular-momentum states are pushed

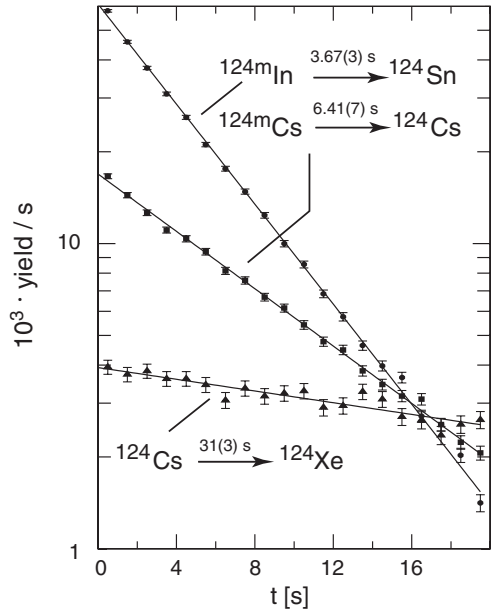

FIG. 4. Decay curves for the ^{124m}Cs isomer and ^{124}Cs g.s. decays and the ^{124m}In β^- decay. The decay curve of the ^{124}Cs g.s. decay (identified by Xe X-rays) is a convolution of the isomer feeding and direct g.s. production. Isomer feeding is, however, too small to be statistically significant.

apart with increasing charge state. Figure 5(a) shows results of these calculations for Cs for different charge states.

Similarly, X-ray intensity ratios $R = K_\beta/K_\alpha$ were determined, which yielded for Sn, $R = 0.21(1)$ [0.172], for Xe, $R = 0.22(2)$ [0.178], and for Cs, $R = 0.21(1)$ [0.179], where the values in square brackets are those for the neutral atoms excluding the $K_{\beta 2}$ transitions [32]. We observed that the measured values did not differ significantly for the two electron-beam energies used for charge breeding. The observed increase of these ratios is consistent with the FAC [31] calculations, which predict a general increase of the K_β/K_α ratios with increasing charge state, as shown in Fig. 5(b) for the Cs case. The calculations yield a ratio of $R = 0.178$ (no $K_{\beta 2}$) for neutral Cs and a value of 0.194 at $q = 32$. An additional increase of this ratio is expected due to the reduction of Auger and shakeoff rates in ions with empty outer shells. Although the increase of the K_β/K_α ratios is significant, it does not appear to affect the nuclear lifetimes or the EC branching ratios. The EC branching ratios are mostly governed by the K, L, and M electron densities at the origin (cf. Ref. [33]), and since the observed shifts are less than a percent of the total electron binding energies, the moderately high charge states in the present experiment will not seriously affect the nuclear decay properties.

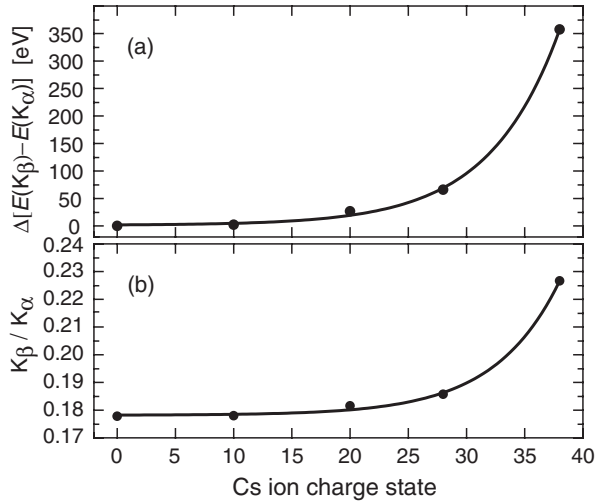

FIG. 5. Relative energy shifts $\Delta[E(K_\beta) - E(K_\alpha)]$ (a) and X-ray intensity ratios $R = K_\beta/K_\alpha$ (b) for Cs ions as a function of charge state. The points represent theoretical calculations, and the solid trend line is an arbitrary function to guide the eye.

In summary, the advantages of using an EBIT as a tool for low-background in-trap X-ray and γ-ray spectroscopy for radioactive ions was demonstrated. Charge breeding was shown to significantly lengthen storage times without ion losses, thereby allowing lifetime measurements of short-lived and medium-long lived radio isotopes. Further, the extra timing information allowed identification of radioactive isobars, which concurrently entered the trap. The high magnetic field of the trap provided an efficient spatial separation between decay photons and decay positrons. A study of atomic properties showed that moderately high charge states do not affect lifetimes or EC branching ratios.

The present technique was developed for the measurement of EC branching ratios of the intermediate odd-odd nuclei in $\beta\beta$ decay, where competing β^--decay branches are orders of magnitude more intense. It can be extended to a variety of high-sensitivity decay measurements on nuclei with low production yields at Radioactive Ion Beam (RIB) facilities, potentially applied with existing or future electron-beam ion traps or sources [34–37].

TRIUMF receives federal funding via a contribution agreement with the National Research Council (NRC) of Canada. We thank the TRIUMF accelerator staff for their support during the course of the present experiment. This work was supported by the Deutsche Forschungsgemeinschaft (DFG) under Grant No. FR 601/3-1 and the National Research and Engineering Council of Canada (NSERC). M. A. acknowledges the financial support from Al-Nahrain University/Ministry of Higher Education and Scientific Research of Iraq. A. T. G. acknowledges support from the NSERC-CGS-D program and T. D. M. from the NSERC-CGS-M program.

*Corresponding author.
Frekers@uni-muenster.de
†Present address: Department of Physics, Stanford University, Stanford, CA 94305, USA.

[1] C. Couratin, Ph. Velten, X. Fléchard, E. Liénard, G. Ban, A. Cassimi, P. Delahaye, D. Durand, D. Hennecart, F. Mauger *et al.*, Phys. Rev. Lett. **108**, 243201 (2012).

[2] G. Li, R. Segel, N. D. Scielzo, P. F. Bertone, F. Buchinger, S. Caldwell, A. Chaudhuri, J. A. Clark, J. E. Crawford, C. M. Deibel *et al.*, Phys. Rev. Lett. **110**, 092502 (2013).

[3] D. Frekers, I. Tanihata, and J. Dilling, Can. J. Phys. **85**, 57 (2007).

[4] S. K. L. Sjue, D. Melconian, A. García, I. Ahmad, A. Algora, J. Äystö, V.-V. Elomaa, T. Eronen, J. Hakala, S. Hoedl *et al.*, Phys. Rev. C **78**, 064317 (2008).

[5] J. Rissanen, J. Kurpeta, V.-V. Elomaa, T. Eronen, J. Hakala, A. Jokinen, I. D. Moore, P. Karvonen, A. Płochocki, L. Próchniak *et al.*, Phys. Rev. C **83**, 011301 (2011);, **83**, 029901(E) (2011).

[6] M. Kowalska, S. Naimi, J. Agramunt, A. Algora, D. Beck, B. Blank, K. Blaum, C. Böhm, C. Borgmann, M. Breitenfeldt *et al.*, Nucl. Instrum. Methods Phys. Res., Sect. A **689**, 102 (2012).

[7] J. Stanja, C. Borgmann, J. Agramunt, A. Algora, D. Beck, K. Blaum, C. Böhm, M. Breitenfeldt, T. E. Cocolios, L. M. Fraile *et al.*, Phys. Rev. C **88**, 054304 (2013).

[8] C. Wrede, S. K. L. Sjue, A. García, H. E. Swanson, I. Ahmad, A. Algora, V.-V. Elomaa, T. Eronen, J. Hakala, A. Jokinen *et al.*, Phys. Rev. C **87**, 031303 (2013).

[9] A. Lapierre, M. Brodeur, T. Brunner, S. Ettenauer, A. T. Gallant, V. Simon, M. Good, M. W. Froese, J. R. Crespo López-Urrutia, P. Delheij *et al.*, Nucl. Instrum. Methods Phys. Res., Sect. A **624**, 54 (2010).

[10] M. C. Simon, J. C. Bale, U. Chowdhury, B. Eberhardt, S. Ettenauer, A. T. Gallant, F. Jang, A. Lennarz, M. Luichtl, T. Ma *et al.*, Rev. Sci. Instrum. **83**, 02A912 (2012).

[11] J. Dilling, R. Baartman, P. Bricault, M. Brodeur, L. Blomeley, F. Buchinger, J. Crawford, J. R. Crespo López-Urrutia, P. Delheij, M. Froese *et al.*, Int. J. Mass Spectrom. **251**, 198 (2006).

[12] K. G. Leach, A. Grossheim, A. Lennarz, T. Brunner, A. T. Gallant, M. Good, R. Klawitter, A. A. Kwiatkowski, T. Ma, T. D. Macdonald *et al.*, arXiv:1405.7209.

[13] V. L. Ryjkov, M. Brodeur, T. Brunner, M. Smith, R. Ringle, A. Lapierre, F. Ames, P. Bricault, M. Dombsky, P. Delheij *et al.*, Phys. Rev. Lett. **101**, 012501 (2008).

[14] M. Smith, M. Brodeur, T. Brunner, S. Ettenauer, A. Lapierre, R. Ringle, V. L. Ryjkov, F. Ames, P. Bricault, G. W. F. Drake *et al.*, Phys. Rev. Lett. **101**, 202501 (2008).

[15] S. Ettenauer, M. C. Simon, A. T. Gallant, T. Brunner, U. Chowdhury, V. V. Simon, M. Brodeur, A. Chaudhuri, E. Mané, C. Andreoiu *et al.*, Phys. Rev. Lett. **107**, 272501 (2011).

[16] M. Brodeur, T. Brunner, C. Champagne, S. Ettenauer, M. J. Smith, A. Lapierre, R. Ringle, V. L. Ryjkov, S. Bacca, P. Delheij *et al.*, Phys. Rev. Lett. **108**, 052504 (2012).

[17] M. Brodeur, T. Brunner, S. Ettenauer, A. Lapierre, R. Ringle, B. A. Brown, D. Lunney, and J. Dilling, Phys. Rev. Lett. **108**, 212501 (2012).

[18] M. Brodeur, V. L. Ryjkov, T. Brunner, S. Ettenauer, A. T. Gallant, V. V. Simon, M. J. Smith, A. Lapierre, R. Ringle, P. Delheij *et al.*, Int. J. Mass Spectrom. **310**, 20 (2012).

[19] A. T. Gallant, J. C. Bale, T. Brunner, U. Chowdhury, S. Ettenauer, A. Lennarz, D. Robertson, V. V. Simon, A. Chaudhuri, J. D. Holt *et al.*, Phys. Rev. Lett. **109**, 032506 (2012).

[20] V. V. Simon, T. Brunner, U. Chowdhury, B. Eberhardt, S. Ettenauer, A. T. Gallant, E. Mané, M. C. Simon, P. Delheij, M. R. Pearson *et al.*, Phys. Rev. C **85**, 064308 (2012).

[21] D. Frekers, M. C. Simon, C. Andreoiu, J. C. Bale, M. Brodeur, T. Brunner, A. Chaudhuri, U. Chowdhury, J. R. Crespo López-Urrutia, P. Delheij *et al.*, Phys. Lett. B **722**, 233 (2013).

[22] S. Ettenauer, M. C. Simon, T. D. Macdonald, and J. Dilling, Int. J. Mass Spectrom. **74**, 349 (2013).

[23] The low-activity primary lead originates from the Britannia Mine in Australia and features at present a ^{210}Pb activity of ≈50 Bq/kg.

[24] National Nuclear Data Center, Brookhaven National Laboratory, http://www.nndc.bnl.gov.

[25] W. H. Walters, J. Rikovska, N. J. Stone, P. Walker, and I. S. Grant, Hyperfine Interact. **43**, 343 (1988).

[26] T. Brunner, M. Smith, M. Brodeur, S. Ettenauer, A. T. Gallant, V. V. Simon, A. Chaudhuri, A. Lapierre, E. Mané, R. Ringle *et al.*, Nucl. Instrum. Methods Phys. Res., Sect. A **676**, 32 (2012).

[27] T. Brunner, A. Lapierre, C. Andreoiu, M. Brodeur, P. Delheji, S. Ettenauer, D. Frekers, A. T. Gallant, R. Gernhäuser, A. Grossheim *et al.*, Eur. Phys. J. A **49**, 142 (2013).

[28] M. C. Simon, T. D. Macdonald, J. C. Bale, U. Chowdhury, B. Eberhardt, M. Eibach, A. T. Gallant, F. Jang, A. Lennarz, M. Luichtl *et al.*, Phys. Scr. **T156**, 014098 (2013).

[29] R. D. Deslattes, E. G. Kessler, Jr., P. Indelicato, L. de Billy, E. Lindroth, J. Anton, J. S. Coursey, D. J. Schwab, C. Chang, R. Sukumar *et al.*, X-ray Transition Energies Database (Version 1.2), National Institute of Standards and Technology, Gaithersburg, MD (2005).

[30] S. Agostinelli, J. Allison, K. Amako, J. Apostolakis, H. Araujo, P. Arce, M. Asai, D. Axen, S. Banerjee, G. Barrand *et al.*, Nucl. Instrum. Methods Phys. Res., Sect. A **506**, 250 (2003).

[31] M. F. Gu, Can. J. Phys. **86**, 675 (2008).

[32] R. Firestone and V. S. Shirley, *Table of Isotopes,* CD-rom (John Wiley & Sons, New York, 1996).

[33] W. Bambynek, H. Behrens, M. H. Chen, B. Crasemann, M. L. Fitzpatrick, K. W. D. Ledingham, H. Genz, M. Mutterer, and R. L. Intemann, Rev. Mod. Phys. **49**, 77 (1977).

[34] P. Delahaye, Nucl. Instrum. Methods Phys. Res., Sect. B **317**, 389 (2013).

[35] M. Grieser, Y. A. Litvinov, R. Raabe, K. Blaum, Y. Blumenfeld, P. A. Butler, F. Wenander, P. J. Woods, M. Aliotta, A. Andreyev *et al.*, Eur. Phys. J. Spec. Top. **207**, 1 (2012).

[36] A. Shornikov, A. Pikin, R. Scrivens, and F. Wenander, Nucl. Instrum. Methods Phys. Res., Sect. B **317**, 395 (2013).

[37] A. Lapierre, S. Schwarz, K. Kittimanapun, J. A. Rodriguez, C. Sumithrarachchi, B. Barquest, E. Berryman, K. Cooper, J. Fogleman, S. Krause *et al.*, Nucl. Instrum. Methods Phys. Res., Sect. B **317**, 399 (2013).